

# JOURNAL OF SCIENCE



SAKARYA UNIVERSITY

## Sakarya University Journal of Science

ISSN 1301-4048 | e-ISSN 2147-835X | Period Bimonthly | Founded: 1997 | Publisher Sakarya University |  
<http://www.saujs.sakarya.edu.tr/>

Title: Role of boron mineral size on thermal, microstructural and mechanical characteristic of IPP

Authors: Uğur Soykan

Received: 2019-10-05 00:29:40

Accepted: 2019-12-10 11:53:42

Article Type: Research Article

Volume: 24

Issue: 1

Month: February

Year: 2020

Pages: 205-219

How to cite

Uğur Soykan; (2020), Role of boron mineral size on thermal, microstructural and mechanical characteristic of IPP . Sakarya University Journal of Science, 24(1), 205-219, DOI: 10.16984/saufenbilder.629629

Access link

<http://www.saujs.sakarya.edu.tr/tr/issue/49430//629629>

New submission to SAUJS

<http://dergipark.gov.tr/journal/1115/submission/start>



## Role of boron mineral size on thermal, microstructural and mechanical characteristics of IPP

Uğur SOYKAN <sup>\*,1</sup>

### Abstract

This study paves to way to investigate the fundamental characteristics including the crystalline melting temperature, percent crystallinity, crystal structure, unit cell parameters, crystal size, mechanical behavior, ultimate strength, Modulus and impact strength in the IPP based composites formed by blending of IPP with the varying content levels (5, 10, 15, 20 and 30%) of ulexites having different particle sizes (45 and 75  $\mu\text{m}$ ). The characterizations of the prepared IPP based composites containing ulexite were performed by means of conventional measurement methods such as Differential Scanning Calorimeter (DSC), X-ray diffractions and several mechanical tests. The obtained results depicted that the content and particle size of boron mineral presenting in IPP based composites had significant effects on the crucial properties of IPP. Namely, the crystalline melting temperature of IPP increased initially (from 165.46°C to 168.54°C) when adding 5% of 45  $\mu\text{m}$  ulexite into IPP and then, dramatic decrease was observed with the content increment. The addition of 75  $\mu\text{m}$  ulexite into to IPP matrix led to consistent decreasing of crystalline melting temperatures of IPP domains. Furthermore,  $a$  and  $b$  unit cell dimensions of monoclinic structures initially showed the expansions. The maxima of  $a$  parameters were found to be 6.683Å and 6.645Å, while the maxima of  $b$  were calculated as 20.845Å and 20.793Å for the 45 $\mu$  and 75  $\mu\text{m}$  ulexites, respectively, but then contracted consistently with the increasing of ulexite content. The serious decrement in  $c$  unit cell parameter was observed with the increasing of ulexite content for the both particle sizes . Moreover, the remarkable reinforcements were achieved in the ultimate strengths (from 24.99 MPa to 31.20 MPa), Young's Modulus (from 369.60 MPa to 516.05 MPa) and impact strength (from 39.56 MPa to 46,68 MPa) of the IPP based composites with 45  $\mu\text{m}$  ulexite. The maximum improvements in mechanical properties were obtained with the composites containing 5% of 45  $\mu\text{m}$  ulexite and mainly 15% of 75  $\mu\text{m}$  ulexite. These developments presumably were caused from advance in the alignments and orientations of the IPP chains in the matrix due to presence of ulexite particles.

**Keywords:** size effect of ulexite mineral, IPP based composites, thermal properties, unit cell parameters, mechanical reinforcement.

\*Corresponding Author: [ugursoykan@ibu.edu.tr](mailto:ugursoykan@ibu.edu.tr)

<sup>1</sup>Yenicaga Yasar Celik Vocational High School, Bolu Abant Izzet Baysal University, Bolu, 14300, Turkey.

## 1. INTRODUCTION

The polymer composite materials (PCMs) have become a significant part of many industrial application areas such as automotive [1], biomedicine [2], aerospace [3], engineering system [4], membrane separation [5], electrical products [6], construction industry [7] etc. They are vastly used with their valuable advantages of the high mechanical strength, corrosive resistance, withstanding prolonged stress, having good processing conditions, good damping characteristics, designing of flexibility [7-10]. Thus, the researchers focused on investigating polymer composites in order to impart the desired properties to the polymers for the proper applications [11]. Isotactic polypropylene (IPP) is the one of the commercially important thermoplastic polymer and have wide usage areas due to its superior characteristics such as extraordinary versatility, low weight, low cost and stability [12, 13]. However, its applications is limited due to some adverse properties such as lack of reactive site, low hydrophobic character, sticking problem, photo oxidation sensitivity and dye uptake etc [14]. At this point, many different kinds of fillers are used for overcoming these drawbacks of the IPP. The mechanical properties [15], processing conditions [16], interfacial morphology [17], conductivity [18], crystallization [19] and thermal behavior [20] of the IPP were improved with the use different kinds of fillers in the polymer matrix.

Recently boron compounds, which their considerable mineral reserves are found in the Turkey and the United States [21], with their particular characteristics have utilized widely in the textile, cleaning, agriculture, bleaching processes, glass and ceramic production as well as nuclear industry, fuel technology and superconductive materials and the production of catalyst [22-25]. Thus, there existed many studies focusing on the evaluation of the boron minerals in the literature. Especially, the boron minerals are used in the polymer composites to enhance their crucial properties such as mechanical, flame retardancy, water absorption etc. [26, 27]. The boron compounds with flame

retardant effect also allow to produce halogen free polymer composites [28]. In addition, among the boron mineral, ulexite ( $\text{NaCaB}_5\text{O}_9 \cdot 8\text{H}_2\text{O}$ ) has a critical role in the insulation technology, fertilizers and the production of borax, boric acid, food preservative, disinfectant, detergents, cosmetic chemical and steel etc [29]. Furthermore, the blending of boron mineral with the thermoplastic polymers have been effective way to upgrade the properties of common thermoplastics. Borazan and coworker [30] prepared the polyester composites containing varying content of both boron compounds (boron oxide, borax pentahydrate and borax decahydrate) and waste pine cone to investigate their mechanical properties. The finding show that the boron compounds gave rise to increase the bending strength and flexural modulus of the composites since the better alignments occurred thanks to improvement of interfacial adhesion between species in the polyester matrix. Ibibikcan and Kaynak [31] investigated that the effect of zinc borate, boron oxide, and boric acid on flame retardant properties of LDPE by using them instead of a certain fraction of aluminium hydroxide in the matrix. They found that the used boron compounds improved the flame retardant characteristics of the composites in the certain levels due to their further contribution to the physical barrier mechanism. Ayrilmis et. al. [32] studied the effect of boron compounds on mechanical, physical and fire properties of propylene-wood composites. The result showed that the composite containing zinc borate had the largest dimensionally stability as well as tensile, Izod and bending strengths. Sen et. al. [33] tried to improve mechanical, thermal and surface characteristics of the thermoplastic polyurethane (TPU) with the use of colemanite as boron mineral. They revealed that the obtained composites depicted good thermal stability due to the increment in both char yield preventing both flame feed and air inlet into the polymer. Moreover, both the glass transition temperatures and mechanical properties of the TPU composites increased with the addition of colemanite into the matrix. Sahin [34] studied the dependence of thermal and mechanical properties of polypropylene on colemanite used

as filler. It was found that the increment in colemanite content raised the elastic modulus and greatly breaking strains of PP composites. However, the thermal expansion coefficient, yield stress and yield strain of the composite materials decreased with the increment in colemanite content.

Despite of many published researches about composite formed by combining of the boron compound with polymers, any study has not been investigate in details the properties of composite containing IPP and ulexites having different micron size. From this point of view, I aimed to fabricate IPP composites having improving properties by using the ulexite with different sizes in this study for the first time. Furthermore, the effects of the addition of different sized ulexites on the thermal, mechanical, microstructural and morphological properties of IPP composites were investigated in details by comparing the neat IPP.

## 2. EXPERIMENTAL METHODS

### 2.1. Materials

Isotactic polypropylene (IPP) coded as MH418 with the density of  $0.905 \text{ g/cm}^3$  was supplied from the Turkish Petrochemical Industry (PETKIM) to use as matrix system. The two types of ground ulexites ( $\text{Na}_2\text{O} \cdot 0.2\text{CaO} \cdot 0.5\text{B}_2\text{O}_3 \cdot 16\text{H}_2\text{O}$ ) possessing 45 and 75  $\mu\text{m}$  sizes were supplied from the Eti Mining Operations General Directorate in Turkey in a 1 kg bags. The chemical composition of used ground ulexite for the fabrication of IPP composites were  $\text{B}_2\text{O}_3$  37.00%, CaO 19.00%,  $\text{SiO}_2$  4.00%,  $\text{SO}_4$  0.25%, As 40 ppm,  $\text{Fe}_2\text{O}_3$  0.04%,  $\text{Al}_2\text{O}_3$  0.25%, MgO 2.50%, SrO 1.00% and  $\text{Na}_2\text{O}$  3.50%.

### 2.2. Preparation of IPP based composites

Granule form of IPP turned into the powder form by dissolving in xylene at boiling temperature and then precipitating with the addition of ethanol. The powder IPP and ulexites (with 45 and 75  $\mu\text{m}$  sizes) were dried at  $50^\circ\text{C}$  under the vacuum for 8 hours before extrusion process.

The composites were obtained by mixing of IPP and ulexite (5, 10, 15, 20 and 30 wt.%) with the use of co-rotating twin screw extruder which is DSM Xplore 15 mL microcompounder. The screw speed and the temperature of the hopper, mixing zone and die of the extruder was kept constant at 100 rpm and  $200^\circ\text{C}$  throughout the extrusion processes for all production of IPP based composites. The composition of all extruded samples were depicted in Table 1.

Table 1. The composition of the prepared composites containing IPP and ulexite.

Samples	IPP (%)	Ulexite (45 $\mu\text{m}$ , %)	Ulexite (75 $\mu\text{m}$ , %)
IPP	100	0	0
IPP0	95	5	0
IPP1	90	10	0
IPP2	85	15	0
IPP3	80	20	0
IPP4	70	30	0
IPP5	95	0	5
IPP6	90	0	10
IPP7	85	0	15
IPP8	80	0	20
IPP9	70	0	30

The extruded samples were moulded both in the dogbone shapes for the tensile tests with the thickness of 2.1 mm, width of 7.6 mm and gauge length of 50 mm. Moreover, the samples having thickness of 1 mm and width of 7 mm were prepared for the impact tests with the help of another mould. Both moulding processes were carried at the temperature of  $220^\circ\text{C}$  for barrel and  $50^\circ\text{C}$  for mould by using DACA Instruments Microinjector with injection pressure of 8.6 bar. The minimum four samples for both tensile and impact tests were prepared for each composition.

### 2.3. Characterization of IPP based composites

Shimadzu TA-60 WS Differential Scanning Calorimeter was utilized for the thermal analyses of the IPP based composites produced. The analyses were carried out with  $10^\circ\text{C}/\text{min}$  heating

rate under nitrogen atmosphere by using 5-15 mg of sample. The heat of fusions values belonging to IPP crystal domains in the IPP based composites were obtained directly from the endotherms of the spectrums by means of the DSC instrument software. The following equation was used for the calculation of the percent crystallinities ( $X_c\%$ ) in IPP matrix:

$$X_c\% = \frac{\Delta H_f}{\Delta H_f^0} \times 100 \quad (1)$$

where,  $\Delta H_f$  is the specific enthalpy of melting (heat of fusion) of IPP crystalline domains in the composite matrix  $\Delta H_f^0$  donates the heat of fusion (209 J/g) of 100% crystalline IPP [35]. XRD patterns of the IPP based composites were investigated by Rigaku Multiflex powder X-ray diffractometer system with  $\text{CuK}\alpha$  target giving a radiation ( $\lambda=1.54^\circ$ ) over the  $2\theta$  range of  $10-60^\circ$ . The XRD analyses were carried out with  $5^\circ/\text{min}$  scanning speed with step increment of  $0.02^\circ$  at the room temperature. The composite samples having same weights were used to compare the sample intensities obtained from XRD patterns. Moreover, both the lattice constants (a,b and c) and grain sizes with the accuracy  $\pm 0.01\text{\AA}$  were determined via the XRD patterns [36]. The tensile properties of the prepared dogbone samples were studied according to the standard of ASTM D-638 with the use of LLYOD LR30K Mechanical Tester with 5 kN load cell at crosshead speed of 5 cm/min. The stress-strain curves of the composite samples were obtained directly from the instrument software during tests. Furthermore tensile strengths, moduli and percent elongation of the IPP based composite samples were determined from these obtained curves. The Izod impact strengths of the unnotched samples were determined by Coesfeld Material Test Pendulum Impact Tester at room temperature according to ASTM standard of D256.

### 3. RESULT AND DISCUSSION

#### 3.1. Thermal analysis of IPP based composites

The effect of ulexite having different sizes on the thermal characteristics of IPP was

investigated by DSC analyses. The thermograms of virgin IPP and the composites containing varying contents (5, 10, 15, 20 and 30) and sizes (45 and 75  $\mu\text{m}$ ) of ulexite were depicted graphically in Figure 1. The endothermic heat flows appearing at both figures was attributed to the melting of IPP crystalline domains [37]. Moreover, the results showed that the crystalline melting temperatures of IPP were highly depended on both the contents and size of the ulexite presenting in the IPP matrix. Namely, at Figure 1.a., the melting temperature belonging to IPP increased initially with the first additional of 45  $\mu\text{m}$  of ulexite and reached the maximum melting temperature value,  $168.54^\circ\text{C}$  with the composites containing 5% ulexite. This increment may be caused from that the ulexite micro particles acted as nucleation accelerators in the IPP matrix, resulting in the larger melting temperature of IPP [38, 39]. That is, the initial addition of the 45  $\mu\text{m}$  ulexite particles gave rise to the advanced in packed ordering of IPP chains, which resulting more ordered structure with the greater chain mobility and alignments of IPP chains. Correspondingly, the obtaining of maximum values in the not only a and b unit cell parameters (Figure 4) but also degree of crytallinity (Figure 2) at this content ( %5 ulexite having 45  $\mu\text{m}$  size) was the experimental evidence to bring about this regular ordering of IPP chains. However, the further addition of 45  $\mu\text{m}$  ulexite to the IPP matrix gave rise to the consistently decreasing of the melting temperature of the IPP and the lowest crystalline melting temperature of IPP,  $165.26^\circ\text{C}$ , was reached at the composite with 30% 45  $\mu\text{m}$  ulexite. The decrement in the melting temperature the domains presumably arising from the formation of microstructural disorders, lattice distortions and defects in the crystal structures of IPP with the increasing of content of 45  $\mu\text{m}$  ulexite in the matrix. Furthermore, the findings obtained from the thermograms belonging to composites containing varying proportional of 75  $\mu\text{m}$  ulexite showed that the crystalline melting temperature of IPP domains gradually decreased with the increasing of ulexite contents in the matrix, Figure 1.b. All prepared composites had the lower melting temperature than that the virgin IPP had. In other

words, the addition of relatively larger ulexite particles to the IPP matrix deteriorated the ordered packing of IPP chains, which caused the decreasing of the crystalline melting temperature of prepared IPP based composites.

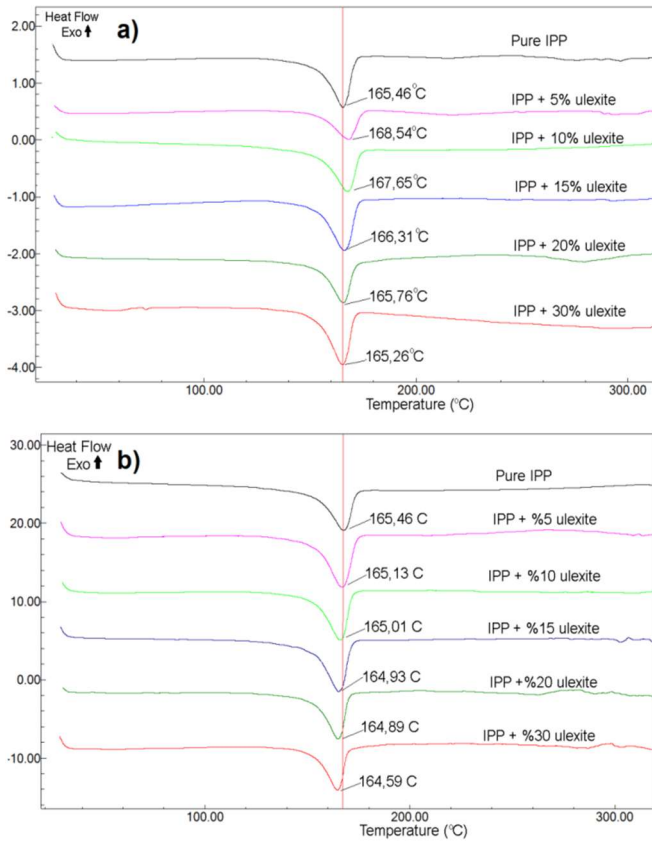


Figure 1. DSC thermogram of virgin IPP and composites formed with various contents of a) 45  $\mu\text{m}$  and b) 75  $\mu\text{m}$  ulexites.

The crystallinities in the IPP matrices of the composites containing both 45 and 75  $\mu\text{m}$  ulexites were determined by using the DSC thermograms and Equation 1. The dependence of crystallinity of the IPP based composites on the size and content of ulexite in the matrix was depicted in the Figure 2. It was seen from the figure that the content and size of the ulexite presenting in the IPP matrix considerably affected the degree of crystallinity characteristics of IPP. The percent crystallinity of the composites containing 45  $\mu\text{m}$  ulexite increased initially and the maxima, 42.56% (15.5% larger than that of virgin IPP) was achieved with the composite containing 5% ulexite. As shown in the results, at this content, the ulexites presenting in the IPP matrix probably gave rise to the

formation of a new fractions of crystallites [40]. Thus, this caused the increment in the degree of crystallinity at this content. However, the further addition of 45  $\mu\text{m}$  of ulexite into the IPP matrix caused the consistent decreasing of the percent crystallinity of the composites [41]. This was attributed that the high content of ulexite in the IPP matrix probably led up the reduction of free volume of the matrix due to filler effect of ulexite. As a result of that, the decrement in the conformational freedom corresponding with free volume caused to limit the crystalline arrangements by hindering of mobility of IPP chains, which resulted in the worse crystallinity. Correspondingly, the minimum value, 30.86% (16.28% smaller than that IPP had) was obtained from the composite with %40 ulexite. In addition to that, at the composites containing varying content of 75  $\mu\text{m}$  ulexites, the degree of crystallinities showed the consistent decreasing trend without any increment. That is, the increment in the content of 75  $\mu\text{m}$  ulexite in the IPP matrix caused the increasing of amorphous character of the IPP. Although the addition of 45  $\mu\text{m}$  ulexite at certain content created the positive effect in term of degree of crystallinity, 75  $\mu\text{m}$  ulexite make the IPP based composites get worse. It was attributed that the presence of the larger particle size and high number of particles in the polymer matrix hinder the progression and growth of the polymer crystals [42]. Accordingly, the obtained result showed that the relatively larger and high content of ulexite particles affected negatively crystallization of the polymer due to the formation of probable heterogeneous nucleations in the matrix, which resulted in decreasing of degree of crystallinity of the IPP based composites.



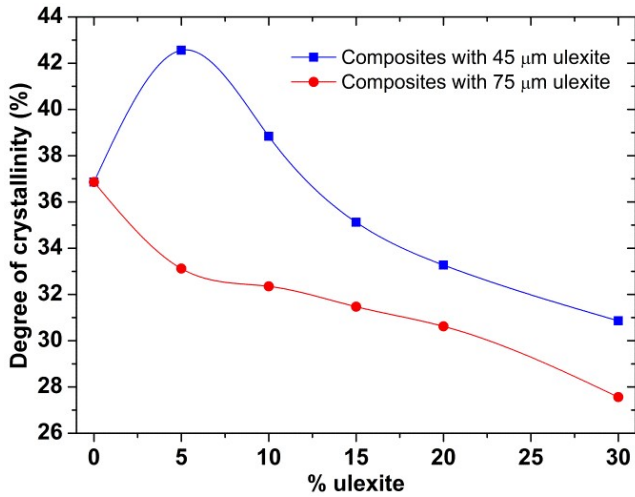


Figure 2. The variation of percent crystallinity ( $X_c$ , %) of the composites with 45 and 75  $\mu\text{m}$  ulexites.

### 3.2. Microstructural properties of IPP based composites

In order to figure out the effects of ulexite particle size and content on the microstructural changes of IPP based composites, XRD analyses of the IPP based composites were carried out. X-ray diffractograms of the composites were graphically recorded at room temperature, as given in Figure 3. The XRD patterns obtained from analyses of the virgin IPP and IPP based composites revealed that the mainly  $\alpha$  form (monoclinic arrangement) and  $\beta$  form (hexagonal arrangements) has been maintained in the crystalline domains. The characteristic diffraction peaks at  $2\theta = 14.1^\circ, 16^\circ, 16.8^\circ, 18.6^\circ, 21.1^\circ$  and  $21.8^\circ$  were observed corresponding to  $\alpha(110)$ ,  $\beta(300)$ ,  $\alpha(040)$ ,  $\alpha(130)$ ,  $\alpha(131)/\beta(311)$ , and  $\alpha(041)$  reflections, Figure 3 [43, 44]. Moreover, the small diffraction peaks detected at about  $29.12^\circ$  was due to the ulexite. Addition to that, it is to be emphasized that observing new appearances, shifts and changes at the diffraction patterns belonging to composites containing both 45 and 75  $\mu\text{m}$  ulexites (Figure 3.a and b) confirmed that the increasing of ulexite contents in the IPP polymer matrix affected negatively to the crystal structures of the IPP. Especially, at 30% ulexite contents, sharpness decrement and disappearing of  $\beta$  form were seen as experimental evidence for the formation of

defects, lattice distortions and microstructural disorders in the crystal structures of IPP matrix [45].

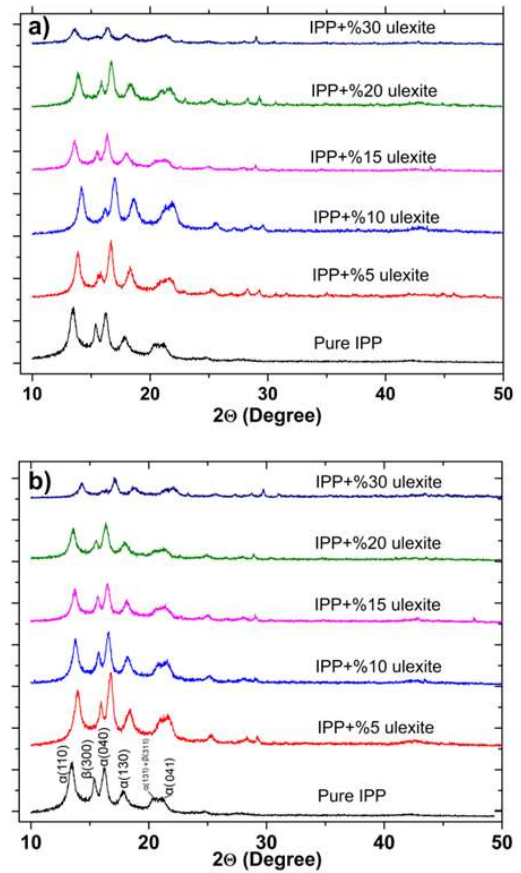


Figure 3. Powder X-ray partial diffraction peaks for virgin IPP and composites with varying contents of a) 45  $\mu\text{m}$  and b) 75  $\mu\text{m}$  ulexites.

The monoclinic unit cell parameters ( $a, b$  and  $c$ ) of the crystalline domains of virgin IPP and IPP based composites were calculated by using XRD diffraction patterns. The calculations were conducted on the basis of a least square method by using  $d$  values obtained directly from the software and 040, 110 and 041 ( $h, k, l$ ) planes. Moreover, the crystal sizes of the virgin IPP and the composites containing ulexite were determined from the XRD pattern with the use of following formula;

$$d = 0.941 \lambda / B \cos \theta_B \quad (2)$$

where  $d$  donates the thickness of crystal,  $\lambda$  implies the wavelength of the used XRD source,  $B$  is FWHM (full width at half maximum) corresponding Bragg peak and  $\theta_B$  donates the

Bragg angle.  $B$  was calculated by using the following formula;

$$B^2 = B_m^2 - B_s^2 \quad (3)$$

where  $B_s$  depicted the half width of the standard material and  $B_m$  the difference between the angles at FWHM of the related peak.

The obtained results as for unit cell parameters showed that the dimensions of the monoclinic unit cells were changed considerably by the addition of ulexites (both 45 and 75  $\mu\text{m}$ ) presenting in the composites. The variations of unit cell parameters  $a$ ,  $b$  and  $c$  on the content of ulexites in the composites were illustrated in Figure 4 in detail. It can be stated that the lateral dimensions ( $a$  and  $b$  unit cell parameters) belonging to composites containing 45 and 75  $\mu\text{m}$  of ulexite showed almost the same trend. Namely, both  $a$  and  $b$  unit cells increased initially and then, the dramatic decreasing was observed in the IPP based composites with both sizes of ulexites. The maximum values for  $a$  and  $b$  unit cell parameters were achieved with the composites containing 5% for 45  $\mu\text{m}$  of ulexite and 15% for 75  $\mu\text{m}$  ulexite. The maxima of  $a$  unit cell parameters were found to be 6.683Å and 6.645Å, while the maxima of  $b$  were calculated as 20.845Å and 20.793Å for the 45 $\mu$  and 75  $\mu\text{m}$  ulexites, respectively. The findings showed that at all contents, the expansion in the lateral dimensions of the IPP based composites containing 45  $\mu\text{m}$  ulexites were larger than that the composites with 75  $\mu\text{m}$  ulexites. This was presumably caused from that 45  $\mu\text{m}$  ulexite particles, which having smaller size, possessed the relatively lower steric effects limiting or hindering to expansion of crystalline regions of IPP chains. Furthermore, the expansions in  $a$  and  $b$  unit cells may be attributed to the increasing of free volumes in the matrix. That is, the initial additions of ulexites probably caused that the components (IPP and ulexite) in the matrix repelled each other due to chemically difference in the nature of components. This allowed IPP chains to be more easily crystallized in the larger free volume to form larger monoclinic units, which resulted from the advance in the ordering of IPP chains, as found in the thermal analysis.

After maxima, the  $a$  and  $b$  unit cell parameters of the IPP based composites containing 45 and 75  $\mu\text{m}$  ulexites depicted sharp decrease with the increasing of ulexite content. Thus, these parameters ( $a$  and  $b$ ) at the composites with 30% of 45 and 75  $\mu\text{m}$  ulexites were reached to lower values than that virgin IPP had, as depicted in Figure 4.a and b. On the other hand, the obtained results revealed that  $c$  cell parameters belonging to IPP based composites with 45 and 75  $\mu\text{m}$  ulexites decreased with the increasing of ulexite contents. All  $c$  cell units calculated were smaller than that virgin IPP had. Since the  $c$  unit cell dimensions was parallel with IPP chains in the monoclinic unit, it remained without any expansion. However, the increasing of ulexites meaning the increasing of compelling and extensive nucleation brought about the consistent decreasing of  $c$  unit cell parameters in the composites with both ulexite sizes.



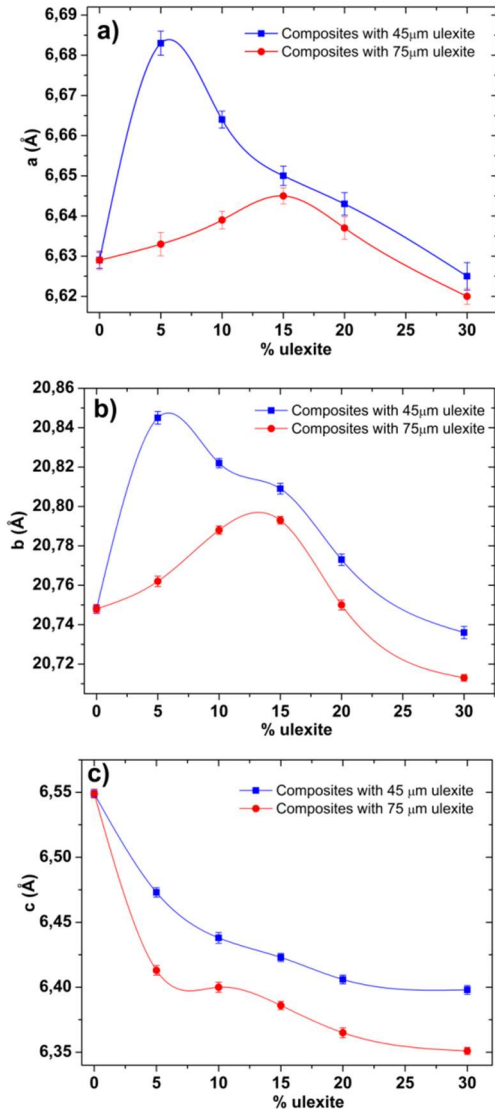


Figure 4. The dependence of a)  $a$ , b)  $b$  and c)  $c$ , unit cell parameters in IPP matrix on 45 and 75 μm ulexite content in the composites.

In addition to unit cell parameters of the prepared IPP based composites, the crystal sizes of virgin IPP and the composites were determined with the use of XRD patterns and Equations 2 and 3. The obtained findings were drawn in Figure 5 as depending on size and content of ulexite in the IPP based composites. It is to be emphasized that the IPP based composites containing both sizes of ulexite showed the different behaviours in term of crystal sizes. Namely, IPP based composites with 45 μm ulexite initially depicted increasing trend then which followed by dramatic decrease with the content whereas the composites with 75 μm ulexite illustrated consistent decreasing with the

increasing of ulexite content. That is, the larger ulexite particles presumably had more heterogeneous nucleation effects on IPP by increasing the overall crystallization rate, which resulting the formation of relatively smaller crystals in the matrix [46]. The obtained results showed good correlation with the unit cell parameters of the IPP based composites containing both ulexite sizes, as seen in Figure 5. It seemed that the variation in the crystal sizes of IPP based composites directly depended on the expansions or contractions observed in the unit cell parameters.

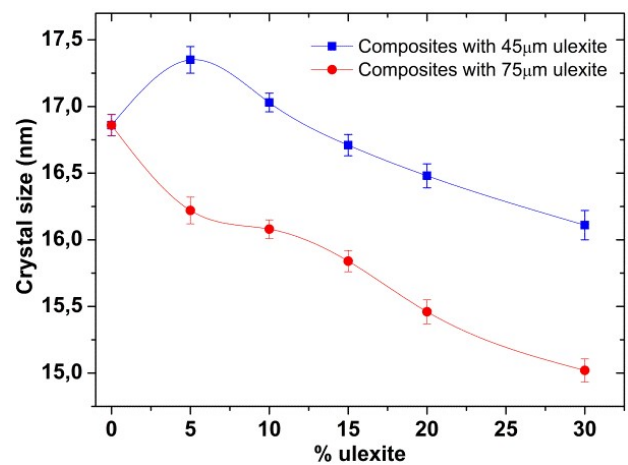


Figure 5. The variation of crystal size of IPP with 45 and 75 μm ulexite contents.

### 3.3. Mechanical characteristics of IPP based composites

The mechanical properties of IPP based composites were studied in order to figure out the effect of ulexite particle size and content on the mechanical behaviour of IPP. The tensile strength, Young's Modulus and impact strength of the IPP based composites were determined via the mechanical tests and the obtained results were numerically tabulated in Table 2.

Table 2. The variation of the mechanical properties of virgin IPP and IPP based composites containing 45 and 75 μm ulexites.

Sample s	Tensile Strength (MPa)	Young's Modulus (MPa)	Impact Strength (kj/m <sup>2</sup> )
IPP	24.99±0.1	369.05±6.3	39.56±0.1
IPP0	31.20±0.2	516.59±4.4	46.68±0.1
IPP1	29.44±0.1	504.45±4.0	45.25±0.2
IPP2	27.78±0.1	492.40±3.9	44.13±0.3
IPP3	27.71±0.2	444.41±4.8	43.63±0.2
IPP4	24.82±0.1	350.12±6.2	38.89±0.3
IPP5	25.20±0.1	405.28±4.3	41.16±0.2
IPP6	25.96±0.1	422.99±3.2	42.87±0.2
IPP7	26.87±0.2	439.77±6.8	41.35±0.3
IPP8	26.65±0.2	432.06±3.9	41.24±0.1
IPP9	23.97±0.4	333.99±5.1	37.21±0.2

Prior to serious discussions on the mechanical properties, it is to be stated that 240°C processing temperature and 8 bar injection pressure were preferred for preparing the composite test sample so as to get away the difficulties in the melt flow and to achieve the ideal dispersion in the matrix. The nominal stress-strain curves belonging to virgin IPP and the composites with varying percentage of 45 and 75 µm ulexites were depicted in detail in Figure 6. Virgin IPP depicted the great extension during cold drawing while all IPP based composites failed at the strain softening regions. As seen in figure, the percent elongation of the IPP based composites containing both size of ulexites decreased with the increasing of the ulexite content in the polymer matrix, which resulted that the composite sample gradually gained brittle nature with ulexite content because the polymer matrices had considerably lower stiffness than rigid inorganic ulexite particles [47]. This presumably was caused from that the rigid properties of the ulexites presenting in the IPP matrix limited or prevented the free movements of IPP chains [48]. Thus the decrements in the strain were obtained with the increment in the ulexite content. On the other hands, the yield strengths and yield points of the IPP based composite samples with both sizes of ulexites increased initially and after maximum, the consistent decrements in the yield strengths and yield points were observed with the increasing of ulexite contents. As depicted in the Figure 6, the maximum yield strengths were found at the IPP composites containing 5%

content of 45 µm of ulexite and 15% content of 75 µm ulexite.

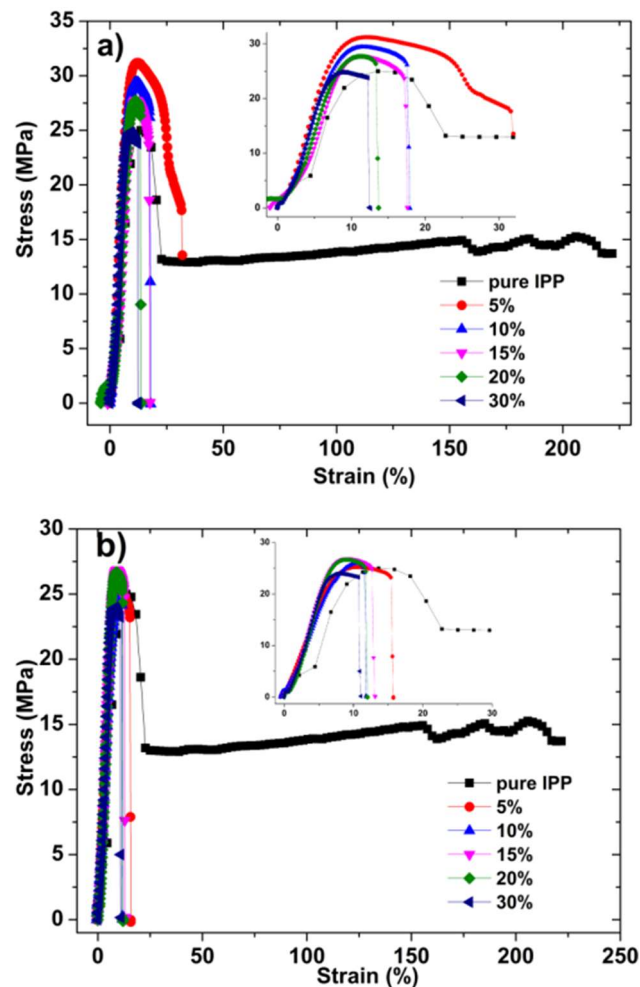


Figure 6. Stress-strain curves of virgin IPP and IPP based composites including varying percentage of a) 45 µm ulexite and b) 75 µm ulexite.

The crucial mechanical properties (ultimate strength, Young's Modulus and impact strength) of the virgin IPP and the composites were investigated in details and the dependence of these characteristic on the size and content of ulexite depicted in the Figure 7. The obtained results revealed that the mechanical properties of the composites were considerably effected by the size and fraction of the ulexite presenting in the IPP polymer matrix. Although the ultimate strength and Young's Modulus showed the almost same trends at both sizes of ulexite, the findings revealed that the ultimate strength and modulus values obtained from the composites containing with 45 µm ulexite were significantly

higher than that the composites with 75  $\mu\text{m}$  ulexites had. That is, the better mechanical properties were obtained for the IPP based composites with the decreasing of the particle size of filler as announced by Tasdemir and Sacaklı [49]. This was presumably caused from that the interfacial adhesion between IPP matrix and ulexite enhanced due to the decrement in the size of the ulexite particle at the same volume fraction, which resulted in the formation of more effective covalent bonds, strong physical interaction and increasing of contact surfaces [50]. As for ultimate strengths, the maximum values were achieved to 31.20 and 26.87 MPa (24.99 and 7.5% improvements with respect to virgin IPP) with the composites containing 5% of 45 $\mu$  and 15% of 75  $\mu\text{m}$  ulexites, respectively, Figure 7.a. On the other hand, the maxima in the modulus belonging to composites with 5% of 45 $\mu$  and 15% of 75  $\mu\text{m}$  was obtained to be 516.59 and 439.77 MPa, respectively, Figure 7.b. After maximum, at both sizes, the ultimate strengths and modulus of the IPP based composites decreased continuously with the increasing of the ulexite contents in the IPP matrix. The ultimate strengths reached the minimum values, 24.82 and 23.97 MPa with the composites including 40% of 45 and 75  $\mu\text{m}$  ulexites, respectively and similarly the minima in the modulus (350.12 and 333.99 MPa) were obtained with the composites including 30% of 45 and 75  $\mu\text{m}$  of ulexites, as seen in Figure 7.a and b. The decrement in both ultimate strength and modulus with the increasing of ulexite content was probably arose from the increasing of rigidity with the addition of ulexite, the acting of further ulexite as impurity in the matrix and the limiting of the alignments of the IPP chains by ulexite particles.

In order to unfold the effect of the ulexite particle size and content on the impact strength of the IPP based composites, Izod impact tests were conducted. The results, which recorded as the energy absorbed by the IPP based composites during the impact tests, were drawn in the Figure 7.c. Only the composites containing 30% of 45 and 75  $\mu\text{m}$  ulexite were broken during impact tests, the composites at other contents showed the ductile behaviours without observing the any

breaks. Among composites, the maximum energy absorptions were found at the composite with 5% of 45  $\mu\text{m}$  ulexite and 10% of 75  $\mu\text{m}$  ulexite. The maxima were recorded as 46.68 and 42.87 MPa for these composites, respectively. It was emphasized that the impact strengths of the composites with 45  $\mu\text{m}$  ulexite were significantly larger than that the composites with 75  $\mu\text{m}$  ulexite had. This was probably caused from that the presenting of more particles having the smaller sizes in the certain region of the polymer matrix provided to be shared relatively more easily the applied sudden stress in the specific region [50]. However, after maxima, the energy absorption capabilities of the IPP based composites decreased with the increasing of the ulexite content in the polymer matrix. The minimum values, 38.89 and 37.21 MPa were recorded with the composites with 30% ulexite in both sizes. The further additions of ulexite into the IPP polymer probably gave rise to restriction of chain mobility. Furthermore, this decrement may be caused from that the formation of agglomerated more microfillers in the IPP matrix led to slippage existing within the agglomerate, which resulted in enhancement of the crack propagation without absorbing more energy [51].

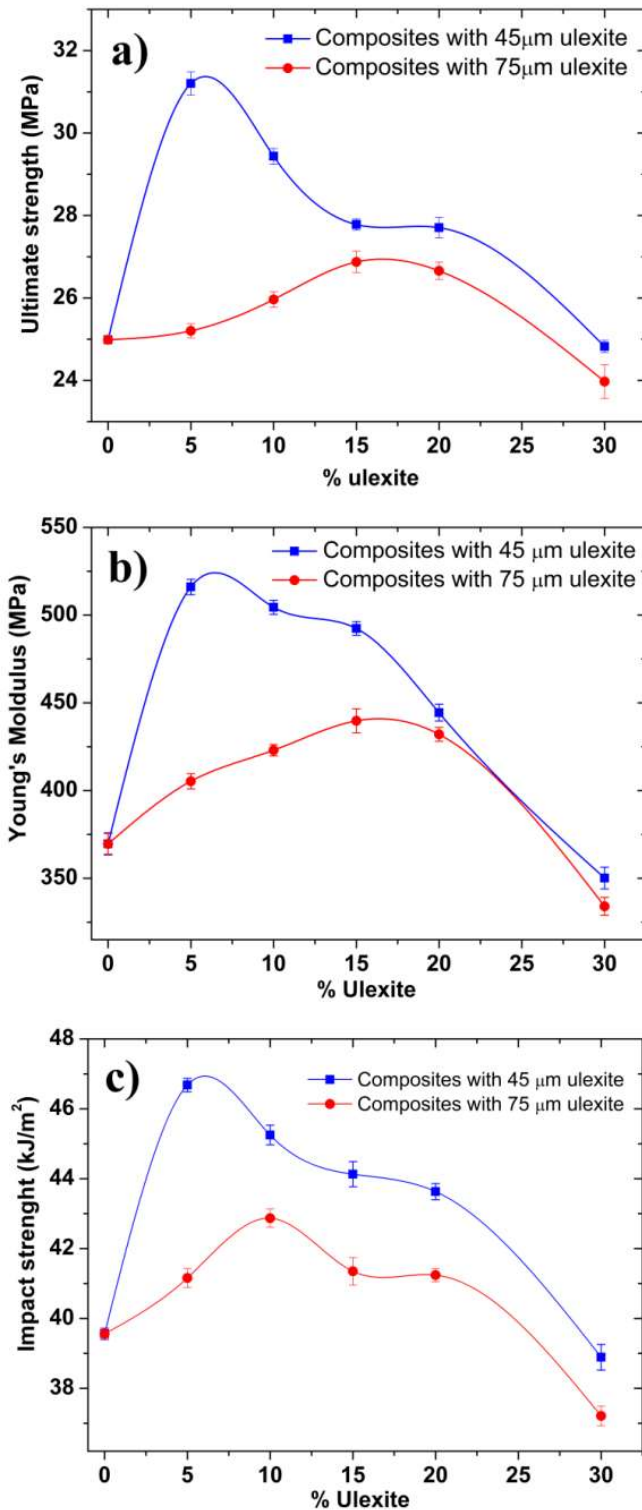


Figure 7. The dependence of a) ultimate strength b) Young's modulus and c) impact strength of the virgin IPP and the composites on the size and content of ulexite.

#### 4. CONCLUSION

In the present work, the role of boron mineral (ulexite) having different particle size and content on the fundamental characteristic features of IPP was investigated in details. The obtained results showed that the thermal, microstructural and mechanical properties of the virgin IPP and composites formed with IPP and ulexite were highly depended on the particle size and fraction of ulexite presenting in the IPP matrix. According to experimental measurements, the optimum ulexite levels were found to be 5% of 45 μm and 15% of 75 μm ulexite for the preparation of IPP based composites having advanced characteristics. The significant conclusions obtained were given as follows;

✓ The additional of ulexite into the polymer matrix resulted in the considerable increase in the crystalline melting temperature of IPP in the composites containing 45 μm ulexites due to the advances in packed ordering of IPP chains. However, the increment in 75 μm ulexite content levels in the IPP based composites led to the consistent decreasing of the crystalline melting temperatures of IPP. As compatible with melting temperatures, at the composites with 45 μm ulexite, the degree of crystallinity increased initially and reached the maximum value with the composites with 5% of ulexite content, and then the dramatic decrements were recorded with the increasing of contents. Furthermore, in the light of the founded results, it was concluded that the addition of 75 μm of ulexite into IPP affected negatively with regard to the percent crystallinities of the prepared composites.

✓ The XRD pattern showed that both  $\alpha$  form (monoclinic arrangement) and  $\beta$  form (hexagonal arrangements) formed in the crystalline domains of IPP. Moreover, the at further content level of 45 and 75 μm ulexite, the crystal structures of the IPP were damaged considerable due to formation of defects, lattice distortions and microstructural disorders. As for monoclinic unit cell parameters of the IPP based

composites,  $a$  and  $b$  unit cell parameters exhibited the increase trends at the certain ulexite levels while  $c$  unit cell parameter decreased seriously with the increasing of ulexite content for the both particle sizes. Moreover, the obtained results depicted that the grain sizes of the IPP based composites had a good correlation with the unit cell parameters.

✓ The findings obtained from mechanical tests revealed that the usage of ulexite as filler in the IPP polymer led to the significant improvements in the tensile strength, Young Modulus and impacts strength. The advances in the alignments and in orientations of IPP chains with the larger chain mobility provided to obtain the reinforced IPP based composites. Furthermore, the obtained results showed that the mechanical properties of IPP based composites were governed by the size of basal areas ( $a \times b$ ) giving rise to increment in the free movements of IPP chains with better alignments instead of the percentage crystallinity.

## 5. ACKNOWLEDGMENTS

This work was supported by department of chemistry at Bolu Abant İzzet Baysal University (BAIBU). Furthermore, the authors especially thanks to chemistry department of Middle East Technical University and Innovative Food Technologies Development Application and Research Center (YENIGIDAM) for valuable supports.

## 6. REFERENCES

- [1] J.C. Lynn, "Polymer composite characterization for automotive structural applications", *Journal of Composites Technology and Research*, vol. 12(4), pp. 229-231, 1990.
- [2] S. Ramakrishna, J. Mayer, E. Wintermantel and K.W. Leong, "Biomedical applications of polymer-composite materials: a review", *Composite Science and Technology*, vol. 61(9), pp. 1189-1224, 2001.
- [3] S. Bhowmik, H.W. Bonin, V.T. Bui and R.D. Weir, "Modification of high-performance polymer composite through high-energy radiation and low-pressure plasma for aerospace and space applications", *Journal of Applied Polymer Science*, vol. 102(2), pp. 1959-1967, 2006.
- [4] J.M. Korde, M. Shaikh and B. Kandasubramanian, "Bionic prototyping of honeycomb patterned polymer composite and its engineering application", *Polymer-Plastic Technology and Engineering*, vol. 57(17), pp. 1828-1844, 2018.
- [5] L.O. Afolabi, P.S.M. Megat-Yusoff, Z.M. Ariff and M.S. Hamizol, "Fabrication of pandanus tectorius (screw-pine) natural fiber using vacuum resin infusion for polymer composite application", *Journal of Materials Research and Technology*, vol. 8(3), pp. 3102-3113, 2019.
- [6] K.M. Vighnesha, Shruthi, Sandhya, D.N. Sangeetha and M. Selvakumar, "Synthesis and characterization of activated carbon/conducting polymer composite electrode for supercapacitor applications", *Journal of Materials Science: Materials in Electronics*, vol. 29(2), pp. 914-921, 2018.
- [7] L. Mohammed, M.N.M. Ansari, G. Pua, M. Jawaid and M.S. Islam, "A review on natural fiber reinforced polymer composite and its applications", *International Journal of Polymer Science*, no. 243947, 2015.
- [8] L. Bilogurova and M. Shevtsova, "Investigation of the improvement of the physical and mechanical properties of polymer composite materials with nano-sized powders", *Materialwissenschaft Werkstofftechnik*, vol. 40(4), pp. 331-333, 2009.
- [9] E. Kuram, "Micro-machinability of injection molded polyamide 6 polymer and glass-fiber reinforced polyamide 6 composite", *Composites Part B-Engineering*, vol. 88, pp. 85-100, 2016.
- [10] S.Y. Duan, F.H. Mo, X.J. Yang, Y.R. Tao, D.S. Wu and Y. Peng, "Experimental and

- numerical investigations of strain rate effects on mechanical properties of LGFRP composite", *Composites Part B-Engineering*, vol. 88, pp. 101-107, 2016.
- [11] X.C. Yin, Y. Li, D. Cheng, Y.H. Feng and G.J. He, "Improvements in thermal conductivity and mechanical properties of HDPE/nano-SiC composites by the synergetic effect of extensional deformation and ISBS", *Journal of Applied Polymer Science*, vol. 136(24), 2019.
- [12] I.K. Mehta, S. Kumar, G.S. Chauhan and B.N. Misra, "Grafting onto isotactic polypropylene .3. gamma-rays induced graft-copolymerization of water-soluble vinyl monomers", *Journal of Applied Polymer Science*, vol. 41(5-6), pp. 1171-1180, 1990.
- [13] H.M. Lee, B.J. Park, I.J. Chin, H.K. Kim, W.G. Kang and H.J. Choi, "Preparation and characterization of PP/organoclay nano composites with maleic-anhydride", *Nanocomposites and Nanoporous Materials*, vol. 119, pp. 203-206, 2007.
- [14] G.S.S. Rao, M.S. Choudhary, M.K. Naqvi and K.V. Rao, "Functionalization of isotactic polypropylene with acrylic acid in the melt: Synthesis, characterization and evaluation of thermomechanical properties", *European Polymer Journal*, vol. 32(6), pp. 695-700, 1996.
- [15] B. Wang, D. Yang, H.R. Zhang, C. Huang, L. Xiong, J. Luo and X.D. Chen, "Preparation of esterified bacterial cellulose for improved mechanical properties and the microstructure of isotactic polypropylene/bacterial cellulose composites", *Polymers-Basel*, vol. 8(4), no. 129, 2016.
- [16] M.F. Mina, S. Seema, R. Matin, M.J. Rahaman, R.B. Sarker, M.A. Gafur and M.A.H. Bhuiyan, "Improved performance of isotactic polypropylene/titanium dioxide composites: Effect of processing conditions and filler content", *Polymer Degradation and Stability* vol. 94(2), pp. 183-188, 2009.
- [17] Q.T. Li, G.Q. Zheng, K. Dai, M.C. Xie, C.T. Liu, B.C. Liu, X.L. Zhang, B. Wang, J.B. Chen, C.Y. Shen, Q. Li and X.F. Peng, "beta-transcrystallinity developed from the novel ringed nuclei in the glass fiber/isotactic polypropylene composite", *Materials Letters* vol. 65(14), pp. 2274-2277, 2011.
- [18] S.L. Huang, Z.Y. Liu, S.D. Zheng and M.B. Yang, "Enhancing the conductivity of isotactic polypropylene/polyethylene/carbon black composites by oscillatory shear", *Colloid and Polymer Science*, vol. 291(12), pp. 3005-3011, 2013.
- [19] D.S. Mi, R.X. La, W.W. Chen and J. Zhang, "Different kinds of transcrystallinity developed from glass fiber/isotactic polypropylene/-nucleation agents composite by microinjection molding", *Polymer for Advanced Technology*, vol. 27(9), pp. 1220-1227, 2016.
- [20] K. Dutt, R.K. Soni and H. Singh, "Thermal stability and crystallization behavior of ter blends of isotactic polypropylene (IPP)/ethylene-propylene diene rubber (EPDM)/nitrile rubber (NBR)", *International Journal of Polymeric Materials*, vol. 61(11), pp. 864-881, 2012.
- [21] M.F. Eskibalci and S.G. Ozkan, "An investigation of effect of microwave energy on electrostatic separation of colemanite and ulexite", *Minerals Engineering*, vol. 31, pp. 90-97, 2012.
- [22] G. Guzel, O. Sivrikaya and H. Deveci, "The use of colemanite and ulexite as novel fillers in epoxy composites: Influences on thermal and physico-mechanical properties", *Composites Part B-Engineering*, vol. 100, pp. 1-9, 2016.
- [23] P.K. Ojha and S. Karmakar, "Boron for liquid fuel Engines-A review on synthesis, dispersion stability in liquid fuel, and combustion aspects", *Progress in Aerospace Science*, vol. 100, pp. 18-45, 2018.
- [24] H. Yetis, F. Karaboga, D. Avci, M. Akdogan and I. Belenli, "Role of novel Mg-coating method on transport properties of



- MgB<sub>2</sub>/Fe wires", *Physica C*, vol. 562, pp. 13-19, 2019.
- [25] S. Tanyildizi, I. Morkan and S. Ozkar, "Nanotitania-supported rhodium(0)nanoparticles: superb catalyst in dehydrogenation of dimethylamine borane", *ChemistrySelect*, vol. 2(20), pp. 5751-5759, 2017.
- [26] D. Kuru, A.A. Borazan and M. Guru, "Effect of chicken feather and boron compounds as filler on mechanical and flame retardancy properties of polymer composite materials", *Waste Management & Research:SAGE Journals*, vol. 36(11), pp. 1029-1036, 2018.
- [27] M. Gecer, E. Baysal, H. Toker, T. Turkoglu, E. Vargun and M. Yuksel, "The effect of boron compounds impregnation on physical and mechanical properties of wood polymer composites", *Wood Res-Slovakia*, vol. 60(5), pp. 723-737, 2015.
- [28] R. Kurt, F. Mengeloglu and H. Meric, "The effects of boron compounds synergists with ammonium polyphosphate on mechanical properties and burning rates of wood-HDPE polymer composites", *European Journal of Wood and Wood Products*, vol. 70(1-3), pp. 177-182, 2012.
- [29] S. Kutuk and T. Kutuk-Sert, "Effect of PCA on nanosized ulexite material prepared by mechanical milling", *Arabian Journal for Science and Engineering*, vol. 42(11), pp. 4801-4809, 2017.
- [30] A.A. Borazan, D. Gokdai, "Pine cone and boron compounds effect as reinforcement on mechanical and flammability properties of polyester composites", *Open Chemistry*, vol. 16(1), pp. 427-436, 2018.
- [31] E. Ibibikcan and C. Kaynak, "Usability of three boron compounds for enhancement of flame retardancy in polyethylene-based cable insulation materials", *Journal of Fire Sciences*, vol. 32(2), pp. 99-120, 2014.
- [32] N. Ayrimis, T. Akbulut, T. Dundar, R.H. White, F. Mengeloglu, U. Buyuksari, Z. Candan and E. Avci, "Effect of boron and phosphate compounds on physical, mechanical, and fire properties of wood-polypropylene composites", *Construction and Building Materials*, vol. 33, pp. 63-69, 2012.
- [33] F. Sen, S. Madakbas, E. Basturk and M.V. Kahraman, "Morphology and mechanical properties of thermoplastic polyurethane /colemanite composites", *Polymer-Korea*, vol. 41(6), pp. 1019-1026, 2017.
- [34] T. Sahin, "Mechanical and thermal properties of colemanite filled polypropylene", *Kgk-Kaut Gummi Kunststoffe*, vol. 64(9), pp. 16-21, 2011.
- [35] H.M. da Costa, V.D. Ramos and M.G. de Oliveira, "Degradation of polypropylene (PP) during multiple extrusions: Thermal analysis, mechanical properties and analysis of variance", *Polymer Testing*, vol. 26(5), pp. 676-684, 2007.
- [36] U. Soykan, S. Cetin, "Reinforcement of high density polyethylene with a side chain LCP by graft copolymerization-thermal, mechanical and morphological properties", *Journal of Polymer Research*, vol. 22(11), 2015.
- [37] S. Cetin, B.O. Sen, U. Soykan, E.E. Firat, G. Yildirim, "Experimental and theoretical approaches for structural and mechanical properties of novel side chain LCP-PP graft coproducts", *Turkish Journal of Chemistry*, vol. 40(3), pp. 467-483, 2016.
- [38] N.L. Severina, Y.S. Yurtseva and M.F. Bukhina, "Contribution of physical and chemical forces of interaction of a polymer with a filler into the crystallization process", *Vysokomol Soedin B*, vol. 25(8), pp. 557-560, 1983.
- [39] M.Z. Rong, M.Q. Zhang, S.L. Pan and K. Friedrich, "Crystallization performance of isotactic polypropylene filled with surface grafting modified nano-silica", *Acta Polymerica Sinica*, vol. 2, pp. 184-190, 2004.
- [40] Z. Bartczak, A.S. Argon, R.E. Cohen and M. Weinberg, "Toughness mechanism in semi-crystalline polymer blends: II. High-density



polyethylene toughened with calcium carbonate filler particles", *Polymer*, vol. 40(9), pp. 2347-2365, 1999.

[41] A. Layachi, A. Makhlof, D. Frihi, H. Satha, A. Belaadi and R. Seguela, "Non-isothermal crystallization kinetics and nucleation behavior of isotactic polypropylene composites with micro-talc", *Journal of Thermal Analysis and Calorimetry*, vol. 138(2), pp. 1081-1095, 2019.

[42] S.C. Tjong, "Structural and mechanical properties of polymer nanocomposites", *Materials Science and Engineering:R: Reports*, vol. 53(3-4), pp. 73-197, 2006.

[43] B.X. Yang, J.H. Shi, K.P. Pramoda and S.H. Goh, "Enhancement of the mechanical properties of polypropylene using polypropylene-grafted multiwalled carbon nanotubes", *Composites Science and Technology*, vol. 68(12), pp. 2490-2497, 2008.

[44] A. Fereidoon, M.G. Ahangari and S. Saedodin, "Thermal and structural behaviors of polypropylene nanocomposites reinforced with single-walled carbon nanotubes by melt processing method", *Journal of Macromolecular Science, Part B*, vol. 48(1), pp. 196-211, 2009.

[45] K.A. Moly, H.J. Radusch, R. Androsch, S.S. Bhagawan and S. Thomas, "Nonisothermal crystallisation, melting behavior and wide angle X-ray scattering investigations on linear low density polyethylene (LLDPE)/ethylene vinyl acetate (EVA) blends: effects of compatibilisation and dynamic crosslinking", *European Polymer Journal*, vol. 41(6), pp. 1410-1419, 2005.

[46] R. Bouza, C. Marco, M. Naffakh, L. Barral and G. Ellis, "Effect of particle size and a processing aid on the crystallization and melting behavior of iPP/red pine wood flour composites", *Composites Part A-Applied Science and Manufacturing*, vol. 42(8), pp. 935-949, 2011.

[47] A. Kasgoz, D. Akin and A. Durmus, "Effects of size and shape originated synergism

of carbon nano fillers on the electrical and mechanical properties of conductive polymer composites", *Journal of Applied Polymer Science*, vol. 132(30), 2015.

[48] A. Pustak, M. Denac, M. Leskovic, I. Svab, V. Musil and I. Smit, "Morphology and mechanical properties of iPP/silica composites modified with (Styrene-b-ethylene-co-butylene-b-styrene) grafted with maleic anhydride", *Polymer-Plastics Technology and Materials*, vol. 54(6), pp. 647-660, 2015.

[49] M. Tasdemir and Y. Sacakli, "The properties of polymer composites filled with Mg(OH)<sub>2</sub> powder", *Journal of Polymer Materials*, vol. 29(2), pp. 189-200, 2012.

[50] Q. Yang, Y.H. Lin, M. Li, Y. Shen and C.W. Nan, "Characterization of mesoporous silica nanoparticle composites at low filler content", *Journal of Composite Materials:SAGE Journals*, vol. 50(6), pp. 715-722, 2016.

[51] A.S. Hamizah, M. Mariatti, R. Othman, M. Kawashita and A.R.N. Hayati, "Mechanical and thermal properties of polymethylmethacrylate bone cement composites incorporated with hydroxyapatite and glass-ceramic fillers", *Journal of Applied Polymer Science*, vol. 125 pp. E661-E669, 2012.